Citation for published version:
Baïri, A, Laraqi, N & Adeyeye, K 2018, 'Thermal behavior of an active electronic dome contained in a tilted hemispherical enclosure and subjected to nanofluidic Cu-water free convection', European Physical Journal Plus, vol. 133, no. 3, 93. https://doi.org/10.1140/epjp/i2018-11914-3

DOI:
10.1140/epjp/i2018-11914-3

Publication date:
2018

Document Version
Peer reviewed version

Link to publication

The European Physical Journal Plus

Thermal behavior of an active electronic dome contained in a tilted hemispherical enclosure and subjected to nanofluidic Cu-Water free convection

--Manuscript Draft--

Manuscript Number:	EPJP-D-17-01262R2
Full Title:	Thermal behavior of an active electronic dome contained in a tilted hemispherical enclosure and subjected to nanofluidic Cu-Water free convection
Article Type:	Regular Article
Corresponding Author:	Abderrahmane Bairi, PhD University ParisX FRANCE
Corresponding Author Secondary Information:	
Corresponding Author's Institution:	University ParisX
Corresponding Author's Secondary Institution:	
First Author:	Abderrahmane Bairi, PhD
First Author Secondary Information:	
Order of Authors:	Abderrahmane Bairi, PhD
	Najib Laraqi, PhD
	Kemi Adeyeye, PhD
Order of Authors Secondary Information:	
Funding Information:	
Abstract:	This study examines the thermal behavior of a hemispherical electronic component subjected to a natural nano-fluidic convective flow. This active dome generates a high power while operating, leading to values of the Rayleigh number reaching 4.56x10^9. It is covered by an isothermal concentric cupola and the space between the hemispheres is filled with a monophasic Water base-Copper nanofluid whose volume fraction varies between 0 (pure water) and 10%. According to the intended application, the disc of the enclosure may be tilted at an angle ranging from 0° to 180° (horizontal disc with dome facing upwards and downwards respectively). The numerical solution has been obtained through the volume control method based on the SIMPLE algorithm. The average temperature of the outer surface of the dome has been determined for many configurations obtained through Rayleigh number variation. The tilt angle of the cavity and the volume fraction vary within wide ranges. The temperature fields presented for several configurations confirm the effects of natural convection. The results clearly highlight the effects of these parameters on the thermal state of the assembly. The study shows that some combinations Rayleigh-tilt angle-volume fraction are incompatible with a normal operating system at steady state and that a thermoregulation is required. The correlation of the temperature-Rayleigh-Prandtl-angle type proposed in this work allows to easily carry out the thermal dimensioning of the considered electronic assembly.

Ref.: Ms. No. EPJP-D-17-01262R2

Thermal behavior of an active electronic dome contained in a tilted hemispherical enclosure and subjected to nanofluidic Cu-Water free convection

The European Physical Journal Plus

Reviewer #1:

The authors have addressed some of the remarks and enriched the introduction and body of the manuscript in this second submission.

Thank you very much. Your comments allow to improve the quality of the manuscript. Your comments have been taken into account in the revised version. The corrections are highlighted in red color in the new version of the manuscript.

Some brief remarks on this version that I believe should be amended:

1. In spite of the explanations given by the authors, I think their definition of Ra continues to be misleading. Using the liquid gap to define Ra has nothing to do with any comparative study on different geometries, as stated by the authors. In the context of this work, it is a measure of the strength of the convective motions. Ra defined as in the article gives a high Ra number regime that has never been reached in the simulations. As an example, with authors definition, a submillimetric hemispheric gap would lead to Ra \sim 1010 with zero convection, which makes no sense.

The work was entirely reconsidered by using the liquid gap as characteristic length to define the Rayleigh Number. The tables and figures have been redone and the correlations have been modified.

2. I reiterate that the election of Maxwell and Brinkmann models makes, in my opinion, this work an iteration of many others in the field. However, now at least the authors discuss the election of these models at the introduction, which is welcome. The reasoning behind supporting these models is as per the authors "The Maxwell model used in many works estimates the thermal conductivity with an uncertainty of the same order of magnitude as the measurements available in the literature". Personally, I think this is an issue related to the use of different experimental methods. Irrespective of that, it would be good to support this claims if the authors include references and discuss them in a well-articulated way, not just include two random references that show a wide discrepancy.

The introduction has been completed.

For me, it is difficult to make a final recommendation. While I think the work has interesting things, I have the impression that this version has looked for a quick fix instead of a more in-depth improvement. I think the authors could address at least the points above, and later it might be ok to recommend it to EPJ+.

Thank you again for the time you spent revising this work and for your interesting comments.

Thermal behavior of an active electronic dome contained in a tilted hemispherical enclosure and subjected to nanofluidic Cu-Water free convection

A. Baïri [1,*], N. Laraqi [1], K. Adeyeye [2]

[1] Université de Paris, Laboratoire Thermique Interfaces Environnement (LTIE), EA 4415, 50, Rue de Sèvres, F-92410 Ville d'Avray, France

[2] University of Bath, Claverton Down, Bath BA2 7AY, UK

Abstract :

This study examines the thermal behavior of a hemispherical electronic component subjected to a natural nanofluidic convective flow. This active dome generates a high power while operating, leading to values of the Rayleigh number reaching 4.56×10^9. It is contained in a hemispherical enclosure and the space between the dome and the cupola is filled with a monophasic Water base-Copper nanofluid whose volume fraction varies between 0 (pure water) and 10%. According to the intended application, the disc of the enclosure may be tilted at an angle ranging from 0° to 180° (horizontal disc with dome facing upwards and downwards respectively). The numerical solution has been obtained through the volume control method based on the SIMPLE algorithm. The average temperature of the outer surface of the dome has been determined for many configurations obtained through Rayleigh number variation. The tilt angle of the cavity and the volume fraction vary within wide ranges. The temperature fields presented for several configurations confirm the effects of natural convection. The results clearly highlight the effects of these parameters on the thermal state of the assembly. The study shows that some combinations Rayleigh-tilt angle-volume fraction are incompatible with a normal operating system at steady state and that a thermoregulation is required. The correlation

[*] Corresponding author Prof. A. Baïri, abairi@u-paris10.fr, bairi.a@gmail.com

of the temperature-Rayleigh-Prandtl-angle type proposed in this work allows to easily carry out the thermal dimensioning of the considered electronic assembly.

Keywords :
Free convection, Copper-Water Nanofluid, Hemispherical cavity, Electronics applications.

Nomenclature

a	thermal diffusivity (m^2s^{-1})
b	exponent defined in Eq. (11)
C	specific heat at constant pressure ($J.kg^{-1}K^{-1}$)
g	gravity acceleration ($m.s^{-2}$)
$\overline{h}$	average convective heat transfer coefficient ($Wm^{-2}K^{-1}$)
$\vec{e}_g$	dimensionless unit vector opposite to the gravity direction (-)
k	coefficient defined in Eq. (11)
m	coefficient defined in Eq. (11)
n	outgoing normal
n^*	dimensionless outgoing normal $n^* = n / R$ (-)
$\overline{Nu}$	average Nusselt Number (-)
p	pressure (Pa)
p^*	dimensionless pressure (-)
P	generated power (W)
Pr	Prandtl Number (-)
q	generated heat flux, $q = P / S_h$ (Wm^{-3})
r	coefficient defined in Eq. (11)
R	radius of the external cupola (m)
Ra	Rayleigh number (-)
R_i	radius of the active, (m)
S_h	exchange area of the active dome (m^2)
T	temperature (K)
T_c	temperature of the external cupola and initial temperature (K)

$\overline{T}$	average temperature of the active dome's surface (K)
T^*	dimensionless temperature (-)
$\left(\overline{T}\right)_{\varphi}$	average dome's surface temperature obtained for $\varphi \neq 0$ (K)
$\left(\overline{T}\right)_{\varphi=0}$	average dome's surface temperature obtained for $\varphi = 0$ (pure water) (K)
$T_{\max}$	maximum temperature of the active dome (K)
$\vec{u}$	velocity vector
$\vec{u}^*$	dimensionless velocity vector
V	volume of the active dome (m^3)
(x, y, z)	Cartesian coordinates (m)

Greek symbols

α	inclination angle of the disc with respect to the horizontal plane (°)
β	volumetric expansion coefficient (K^{-1})
$\overline{\delta}$	temperature difference $\overline{\delta} = \left(\overline{T}\right)_{\varphi} - \left(\overline{T}\right)_{\varphi=0}$ (K)
$\overline{\Delta T}$	difference of temperature ; $\overline{\Delta T} = \overline{T} - T_c$ (K)
$\vec{\nabla}^*$	dimensionless nabla operator (-)
∇^{*2}	dimensionless Laplacian operator (-)
φ	volume fraction (%)
λ	thermal conductivity ($Wm^{-1}K^{-1}$)
μ	dynamic viscosity (Pa.s)
ρ	density ($kg.m^{-3}$)

Subscripts

f	base fluid (pure water)
h	active dome
nf	nanofluid
s	solide nanoparticles

1. Introduction

Hemispherical cavities are used in various engineering sectors such as nuclear techniques, solar energy, surveillance and security, lighting and building. This geometry is also used for the thermoregulation of electronic assemblies through natural convection considered in this work. Recent work has been devoted to this field with air-filled hemispherical enclosures [1-4] whose active base (disc) is subjected to various thermal boundary conditions (Neuman, Dirichlet) corresponding to different actual operations. For some applications, this base is tilted with respect to the horizontal plane between 0° (horizontal disc with dome facing upwards) and 180° (horizontal disc with dome facing downwards). The dynamic and thermal phenomena occurring in each case are detailed in the works cited above. Correlations of the Nusselt-Rayleigh type are proposed to determine the convective heat transfer corresponding to each configuration. They are synthesized in [5]. Some studies examine the thermal behavior of the active disk and correlations are proposed to calculate its surface temperature. Previous studies examine some aspects of the natural convective flows occurring in hemispherical cavities filled with fluids other than air. This is the case of [6] which considers a hemispherical assembly consisting of an active dome maintained isothermal and a horizontal active disk. The cavity is filled with a fluid whose Prandtl number varies between 6 and 13000. Natural convective heat exchanges are quantified by means of correlations of the Nusselt-Rayleigh-Prandtl type reduced to Nusselt-Rayleigh type. This shows that the thermophysical characteristics of the used fluid have no influence on convective heat transfer. Many other studies such as [7,8] applied to the field of nuclear techniques come to the same conclusion: the fluid's quality has no effect on the convective heat transfer. Nanofluids are homogeneous mixtures consisting of a base fluid and high thermal conductivity nanoparticles. These are used in applications aimed at enhancing natural convective transfer in assemblies generating an important heat flux. The present work specifically deals with the electronics sector in which the generated volumetric heat flux could reach many GWm^{-3}. Many documents such as [9-12] offer information about composition, manufacturing techniques, fields of application and physical characteristics of these nanofluids. Some reviews [13-15] are devoted to nanofluidic natural convection as an abundant scientific production is devoted to them recently, dealing with various aspects. The latter show that several physical parameters influence the dynamic and thermal characteristics of the convective flow. Among the most impacting ones stand the geometry and dimensions of the enclosure, the position of the active parts with respect to the field of gravity, the presence of obstacles, their shape and dimensions, the generated power and temperature. The composition of the used nanofluid (base fluid, nanoparticles, volume fraction) plays an important role in heat exchanges. However, the conclusions of the studies dealing with natural convection through nanofluids are very different with regard to the enhancement of convective heat transfer [16-18]. The survey [19] deals with natural convection using a water-base Copper nanofluid contained in a square cavity including a heat-generating square solid. The study shows that average Nusselt Number representing the convective heat transfer increases of about 27% with increasing nanofluid volume fraction. The latter varies between 0 and 8% when the Rayleigh number is lower than 10^5. Nevertheless, enhancement is only of 9.5% for a Rayleigh number higher than 10^7. By using the water-base CuO nanofluid, the same conclusion is reached in [20] dealing with the case of a rectangular cavity with two vertical walls differentially heated and in [21] examining a Rayleigh-Bénard convection where the better enhancement corresponds to low Rayleigh number of 10^3. The study [22] also shows that the convective heat transfer through Copper-Water nanofluid is improved when the volume fraction increases in the 10^3-10^5 Grashof Number range. The tilt angle with respect to the gravity field significantly influences the free convective heat transfer. This aspect is confirmed in works concerning various forms of cavities such as [23, 24] dealing with a square cavities filled with a water-base Al_2O_3 nanofluid and in [25] using the same nanofluid and the TiO_2–water in an inclined pipe. The choice of nanofluid model is very important to quantify heat transfer in the considered assembly, as confirmed by many works published in this area. According to the considered nanofluid, its thermophysical characteristics and fraction volume as well as other physical parameters, some works cited previously show that heat transfer is improved in some cases. However, it remains almost unchanged and is even decreased for some combinations, proving that the use of nanofluids is not always effective.

Several models are proposed in many works to calculate the effective dynamic viscosity and thermal conductivity of various nanofluids. The excellent technical note [26] contains an interesting review on this subject. Based on data from available experimental works, the author proposes empirical correlations to better estimate the effective dynamic viscosity and thermal conductivity of nanofluids. As stated by the author, these essential characteristics depend on several physical parameters such as the nanoparticle diameter and the temperature of the suspension for the effective thermal conductivity which is either under or over-estimated by the Maxwell equation used in the present work. The Maxwell model used in many works estimates the thermal conductivity with an uncertainty of the same order of magnitude as the measurements available in the literature. This model thus appears to be suitable for the water-based Copper nanofluid work considered in this work. This comment remains valid for the

Brinkman model concerning the viscosity. A state of the art concerning the thermal conductivity and viscosity models is presented in the recent work [27]. This interesting review clearly shows that the perfect models do not exist today and that research must continue in this area, particularly through the experimental approach, by examining the influence of many physical parameters. Research is currently very active in this field [28-30] and will soon lead to reliable models for these important thermophysical characteristics, thus making it possible a better modeling of the convective phenomena with nanofluids. Some recent studies are devoted to the natural convective phenomena occurring in the hemispherical cavities. The work [31] deals with the case of a hemispherical cavity filled with water-base ZnO nanofluid and containing an active cubic electronic device. The same cavity whose base (disc) is active and filled with the same nanofluid is treated in [32]. In both studies, the base of the cavity is inclined by an angle varying between 0 and 180° (dome oriented upwards and downwards respectively) by steps of 15°. The correlations of the Nusselt-Rayleigh-Prandtl-tilt inclination type proposed in these studies allow calculating the convective heat exchanges for several configurations in wide Rayleigh ranges. The study [33] quantifies the convective heat transfer with a water-base Copper nanofluid contained between two concentric hemispheres. One is active and the other is kept isothermal, being the base of the assembly inclined between 0 and 180° with respect to the horizontal plane. The present work completes that study by examining the thermal behavior of the inner dome which generates power in a wide range resulting in high Rayleigh numbers up to 7.29×10^{10} corresponding to specific applications. The volume fraction of the monophasic water-base Copper nanofluid varies between 0 (pure water) and 10%. The numerical study done by means of the volume control method based on the SIMPLE algorithm confirms the effectiveness of the nanofluid for cooling purposes of the active hemispherical electronic component. Its average surface temperature decreases as the fraction volume increases. The temperature reduction may exceed 7K for some combinations Rayleigh-tilt angle-volume fraction. The study also shows that thermoregulation is necessary to avoid consequences incompatible with normal operation of the assembly. These may be boiling, degradation of the nanofluid properties or maximum admissible temperature exceeding for electronic components. An easy method to apply correlation is proposed, allowing to calculate the average surface temperature of the active component used in various engineering fields.

2. The treated assembly

The hemispherical electronic component of radius R_i presented in Fig. 1(a) is soldered to the center of a disc of radius $R = 2R_i$ which constitutes the basis of the assembly. It is covered by concentric cupola maintained isothermal at temperature $T_c = 300\,\text{K}$ and the space between the hemispheres is filled with a monophasic Water base-Copper nanofluid whose volume fraction varies between 0 (pure water) and 10%. According to the intended application, the disc of the enclosure may be tilted at an angle ranging between 0° and 180° (horizontal disc with dome facing upwards and downwards respectively as represented in Fig. 1(b). The outer face of the disk is thermally insulated (adiabatic).

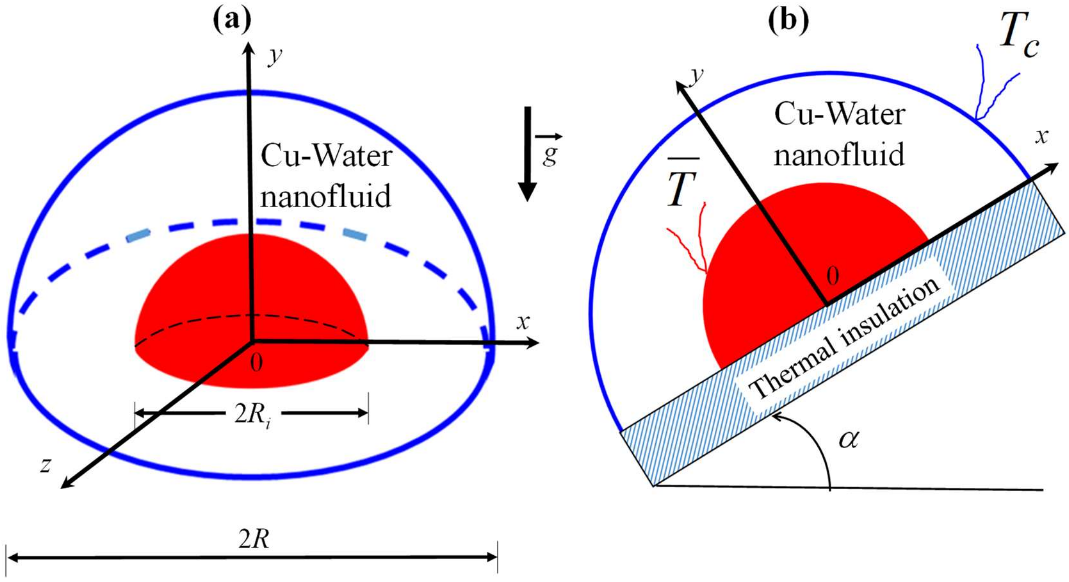

Figure 1. The nanofluid-filled and tilted hemispherical enclosure with its active dome

During operation, the active dome of thermal conductivity λ_h generates a uniform power P. The average temperature of its external surface S_h subjected to the natural convective phenomena is denoted as $\overline{T}$. The thermophysical characteristics (conductivity, density, specific heat and volumetric expansion coefficient) of the Copper nanoparticles (subscript s) are presented in Table 1. The same physical parameters complemented by the dynamic viscosity concerning the pure Water (subscript f) are presented in Table 2.

Table 1. Thermophysical characteristics of the Copper nanoparticles [19]

λ_s ($Wm^{-1}K^{-1}$)	ρ_s ($kg.m^{-3}$)	C_s ($J.kg^{-1}K^{-1}$)	β_s (1/K)
401	8933	395	$1.67x10^{-5}$

Table 2. Thermophysical characteristics of the pure Water [19]

λ_f ($Wm^{-1}K^{-1}$)	ρ_f ($kg.m^{-3}$)	C_f ($J.kg^{-1}K^{-1}$)	β_f (1/K)	μ_f (Pa.s)
0.613	997	4180	$2.1x10^{-4}$	$8.91x10^{-4}$

These data allow to calculate the characteristics of the resulting monophasic nanofluid by using the following models [19, 22] (Maxwell for the effective thermal conductivity and Brinkman for the effective viscosity), according to the considered volume fraction φ .

$$\lambda_{nf} = \left[\frac{\lambda_s + 2\lambda_f - 2\varphi(\lambda_f - \lambda_s)}{\lambda_s + 2\lambda_f + \varphi(\lambda_f - \lambda_s)} \right] \lambda_f \ ;$$

$$\mu_{nf} = \frac{\mu_f}{(1-\varphi)^{2.5}} \ ;$$

$$\rho_{nf} = (1-\varphi)\rho_f + \varphi\rho_s \ ; \tag{1}$$

$$C_{nf} = \frac{(1-\varphi)(\rho C)_f + \varphi(\rho C)_s}{\rho_{nf}} ;$$

$$\beta_{nf} = \frac{(1-\varphi)(\beta\rho)_f + \varphi(\beta\rho)_s}{\rho_{nf}}$$

The values of the Prandtl Number Pr

$$\Pr = \left(\frac{\mu C}{\lambda} \right)_{nf} \tag{2}$$

corresponding to the six φ values considered in this work (0, 1, 3, 5, 7.5, 10%) are presented in Table 3.

Table 3. Considered φ and Pr values for the Water base-Copper nanofluid

φ	0%	1%	3%	5%	7.5%	10%
Pr	6.074	5.592	4.822	4.236	3.679	3.254

3. Numerical solution, governing system

The considered problem is governed by the following dimensionless system written in vector form, detailed in several documents [35,36]

$$\text{Continuity}: \vec{\nabla}^* \vec{u} = 0$$

$$\text{Momentum}: \left(\vec{u}^* \vec{\nabla}^*\right)\vec{u}^* = -\vec{\nabla}^* p^* + \Pr \nabla^{*2} \vec{u}^* + Ra \Pr T^* \vec{e}_g \tag{3}$$

$$\text{Energy}: \vec{u}^* \vec{\nabla}^* T^* = \nabla^{*2} T^* \text{(fluid)};\ \nabla^{*2} T^* = 0 \text{ (cupola)}$$

where $\vec{\nabla}^*$, ∇^{*2} and $\vec{e}_g$ are the nabla operator, the Laplacian spherical operator and the unit vector opposite to the gravity direction respectively, while the dimensionless velocity vector $\vec{u}^*$ and pressure p^* are defined as

$$\vec{u}^* = \frac{\vec{u}R}{a}\ ;\ p^* = \frac{R^2 p}{\rho a^2} \tag{4}$$

being $a = \lambda/\rho C$ the thermal diffusivity, while the dimensionless temperature T^* is defined with

$$T^* = \left[\frac{T - T_c}{\frac{qR}{\lambda_{\text{nf}}}}\right] \tag{5}$$

The Rayleigh Number Ra is based on the liquid gap $\left(R - R_i\right) = R_i$ as characteristic length and the uniform heat flux $q = P / S_h$ generated by the active dome

$$Ra = \left(\frac{\beta\rho}{\mu\lambda a}\right)_f gR_i^4 q \tag{6}$$

The volume control method used here and presented in [35,36] is associated to the SIMPLE algorithm. The unstructured mesh of the computational domain presented in Fig. 2 is composed of tetrahedral volumetric elements and triangular surface elements.

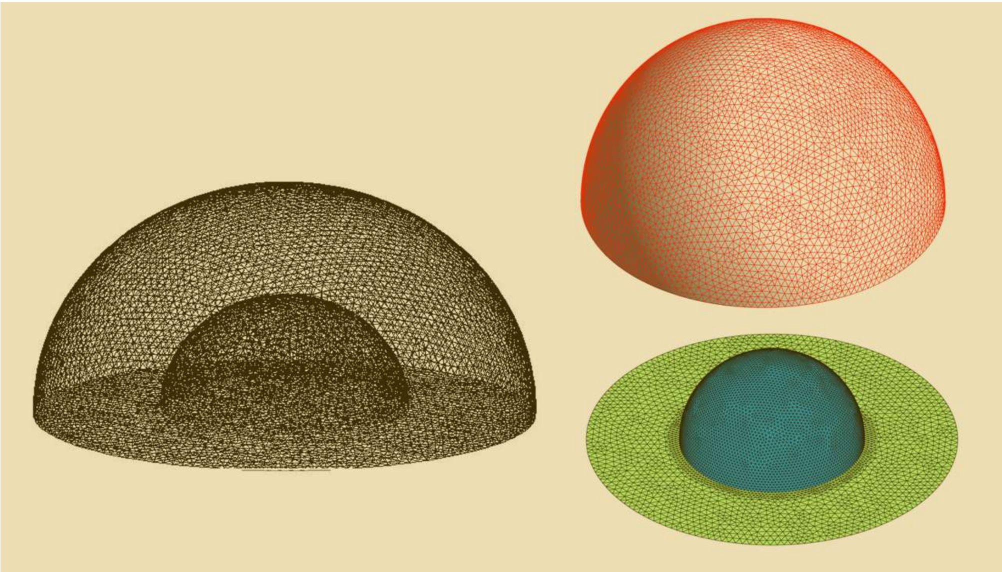

Figure 2. The adopted mesh for the considered assembly

A refinement of the mesh was carried out in the vicinity of the surfaces in contact with the fluid. This is required in order to take into account the variation of the nanofluid thermal characteristics versus the volume fraction, including the effects of viscosity on the dynamic and thermal characteristics of the boundary layer. This also makes it possible to calculate with precision the parietal thermal gradients and the distribution of the temperature on the surface S_h of the active dome of the assembly, the main objective of the present work.

Initial dynamic and thermal boundary conditions are that the fluid is stationary. In addition, the entire computational domain including the nanofluid, the hemispheres and the disc is considered isothermal at temperature $T_c = 300\text{K}$. Throughout the calculation process, the dynamic no-slip condition is imposed on all the surfaces of the domain in contact with the nanofluid, the external dome is kept isothermal $\left(T^* = 0\right)$, the outer face of the disk is adiabatic (perfect insulation) and the active dome generates a uniform heat flux q. Moreover, the condition of continuity of the flux and of the temperature at the fluid-solid interface

$$\lambda_{\text{nf}}\left(\frac{\partial T^*}{\partial n^*}\right)_{\text{nf}} = \lambda_{\text{s}}\left(\frac{\partial T^*}{\partial n^*}\right)_{\text{s}} \ ; \ \left(T^*\right)_{\text{nf}} = \left(T^*\right)_{\text{s}} \tag{7}$$

is imposed. A heat balance is systematically carried out in steady state on the hot and cold surfaces (dome and dome respectively) for all the configurations processed. The convergence of the numerical solution obtained by means of a home-made software is considered to be reached when the relative deviation between the results of two successive iterations are lower than 10^{-5} for the velocity components and 10^{-6} for the energy. Preliminary calculations were carried out to optimize the mesh and control the mesh independence solution. They are done with an unfavorable configuration from the point of view of calculation time which corresponds to the horizontal cavity with the dome facing upwards $(\alpha = 0)$, associated to the maximal Ra and $\Pr$ values. This work based on the field of temperature was carried out with an initial mesh of 342,812 elements which was increased by steps of 2%. The chosen mesh ensures a variation of the temperature of less than 0.5% after 3 successive increases of the mesh. This condition was obtained with 571,422 elements. This mesh has been preserved for all (Ra,α,φ) configurations processed.

4. Results

Various configurations have been calculated by combining *(i)* 10 Ra values presented in Table 4 corresponding to the generated power P between 0.5 and 700W *(ii)* 13 α values varying between 0 and 180° by steps of 15° and *(iii)* 6 φ values of Table 2 (0, 1, 3, 5, 7.5 and 10%).

Table 4. Considered Ra values

P (W)	0.5	5	10	50	100
Ra	3.25×10^6	3.25×10^7	6.51×10^7	3.25×10^8	6.51×10^8

P (W)	200	300	400	500	700
Ra	1.30×10^9	1.95×10^9	2.60×10^9	3.25×10^9	4.56×10^9

Fields of the dimensionless temperature T^* in (*x,y*) and (*x,z*) planes for the nanofluid are presented in Fig. 3 for $\varphi = 5\%$, $Ra = 1.04 \times 10^9$ and $\alpha = 0,45,90,135,180°$.The dynamic and thermal phenomena concerning the natural convective flow taking place in the interstice between the two hemispheres as well as details of the corresponding convective heat transfer are presented in [33].

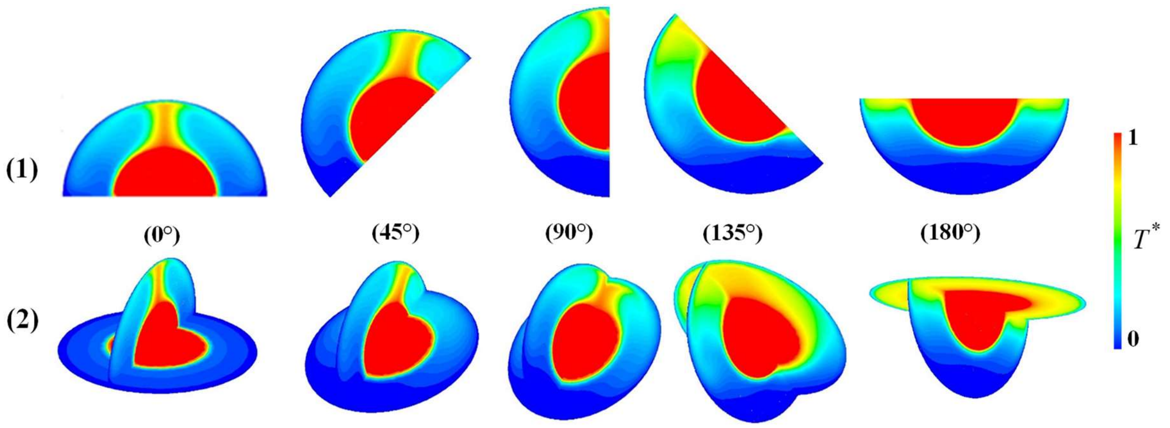

Figure 3. Fields of the dimensionless temperature T^* **(1)** in (*x,y*) plane; **(2)** in (*x,y*) and (*x,z*) planes for $\varphi = 5\%$, $Ra = 1.04 \times 10^9$ and $\alpha = 0,45,90,135,180°$

The temperature fields in the (x, y) plane presented in Fig 3 (1) confirm that the hottest zones are systematically located in the upper parts of the cavity, for any (Ra, α, φ) combination. These fields influence those of the disk as clearly shown in Fig 3(2). The distribution is axisymmetric when the active dome is horizontal with the dome facing upwards $(\alpha = 0)$ and downwards $(\alpha = 180°)$. The maximum and average temperature values decrease as φ increases, which highlight the influence of nanofluid on natural heat convective exchanges and its effectiveness on active dome cooling. When the cavity is inclined, the components of the total buoyancy force are different on the 3 coordinates and the dynamic phenomena are then modified. The nanofluidic thermal field is then no longer axisymmetric, which influences the surface temperature of the dome. On a large part of the disc not covered by the active dome, a quasi-stratification is observed for the lowest considered Ra value (5.21×10^7) when $\alpha = 180°$. In this case, the fluid activity is low in a large part of the interstice.

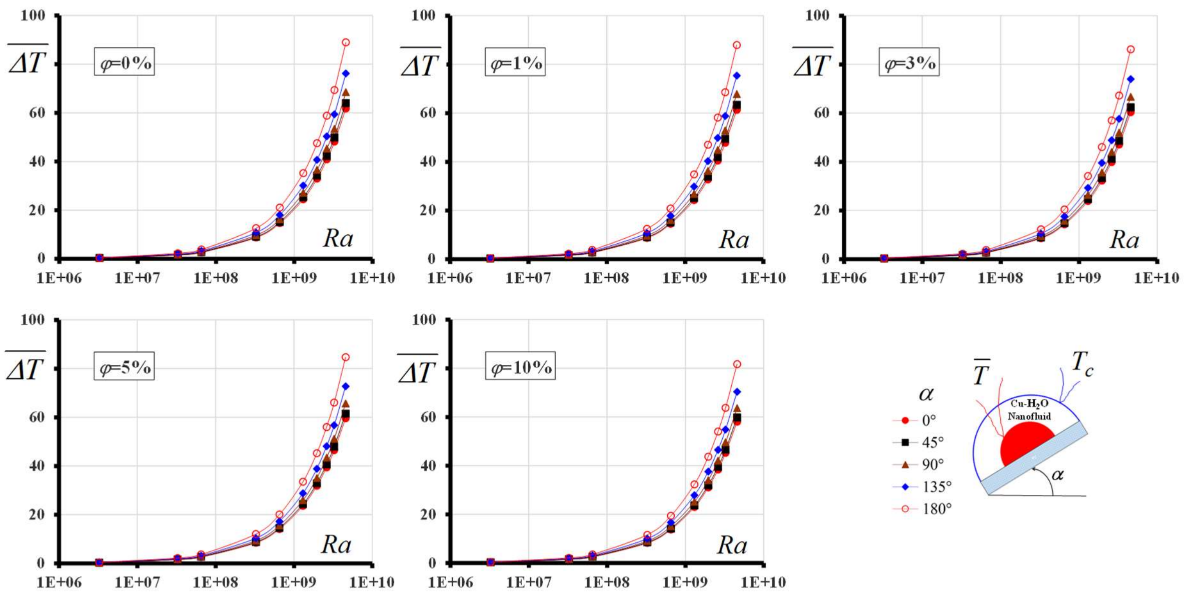

Figure 4. Evolution of the difference temperature $\overline{\Delta T}$ versus Ra for $0 \le \varphi \le 10\%$ and $0 \le \alpha \le 180°$

The difference between the average temperature of the dome $\overline{T}$ and that of the cupola $T_c = 300\,\mathrm{K}$

$$\overline{\Delta T} = \overline{T} - T_c \tag{8}$$

was determined for all cases. It is presented versus Ra in Fig. 4 for some representative φ values varying between 0 (pure water) and 10%, and five tilt angles α between 0 and 180°.

The increase of $\overline{\Delta T}$ versus Ra is systematic for all (φ,α) combinations and the evolution shows a clear decrease in $\overline{\Delta T}$ as Pr increases (φ decreases).

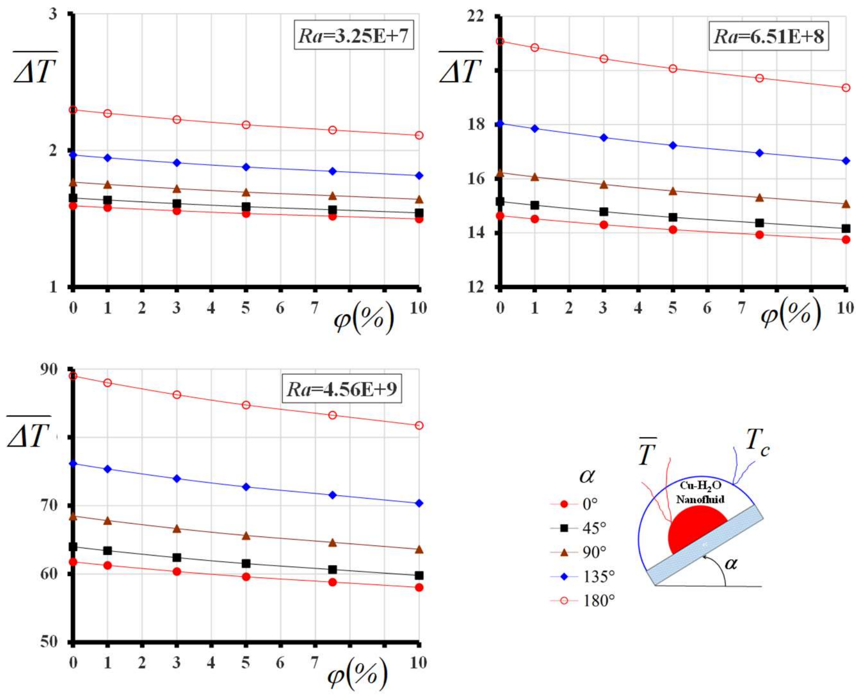

Figure 5. Evolution of the difference temperature $\overline{\Delta T}$ versus the volume fraction φ for some Ra values and tilt angle $0 \le \alpha \le 180°$

These trends are confirmed in Fig. 5 which also shows that the minimum difference $\overline{\Delta T}$ corresponds systematically to $\alpha = 0°$ while the maximum value concerns the cavity with the oriented dome downwards $(\alpha = 180°)$. These effects are detailed in Fig. 6 in the overall Ra range. For some (Ra,φ,α) combinations, the temperature may reach high values incompatible with the correct operation of the electronic assembly. They can have various consequences such as

- nanofluid boiling;
- exceeding the maximum temperature recommended by the manufacturers for the electronic component. Maximum temperature of the dome T_{max} is reached at $(x=0, y=0, z=0)$. The temperature difference $(T_{max} - \overline{T})$ depends on the thermal conductivity of the dome λ_h, its radius R_i and the generated heat flux q. It can reach

2-3K, added to the $\overline{\Delta T}$ value. The maximum permissible temperature can thus be exceeded for large Ra values and large tilt angles α;

- early aging and even deterioration of the physical state of the nanofluid since the temperature affects its characteristics [37,38].

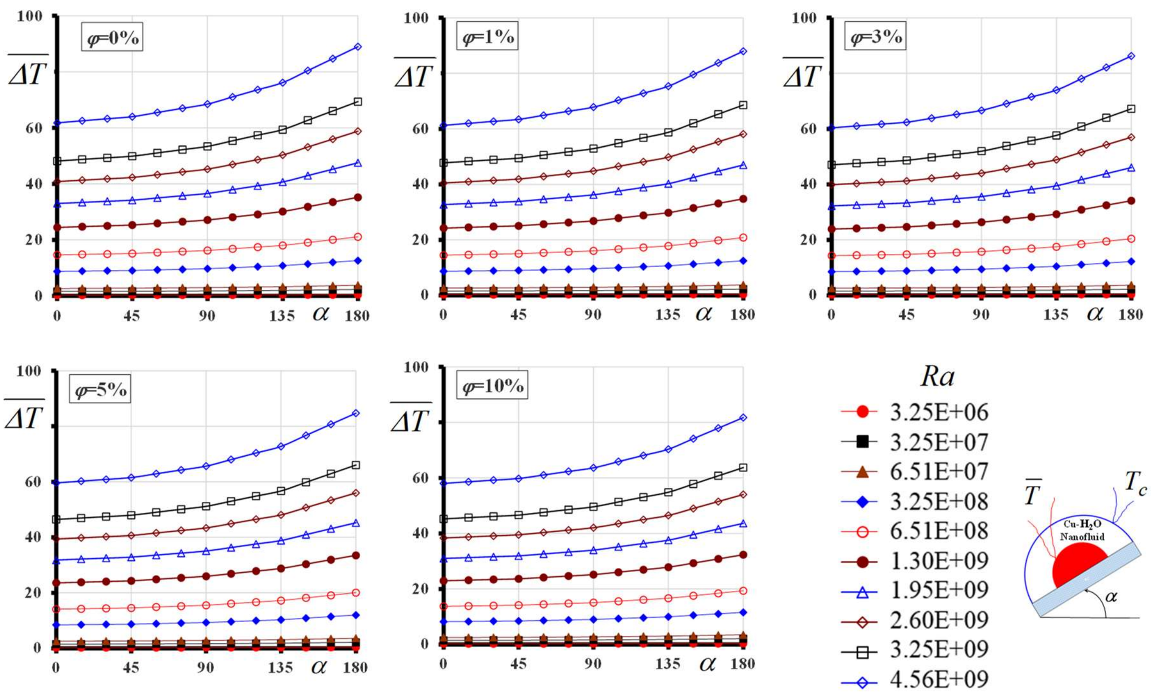

Figure 6. Evolution of the difference temperature $\overline{\Delta T}$ versus the tilt angle α for $3.25\text{x}10^6 \leq Ra \leq 4.56\text{x}10^9$ and $0 \leq \alpha \leq 180°$

The surface average temperature of the dome obtained for a given value of the volume fraction $\varphi \neq 0$ denoted as $\left(\overline{T}\right)_\varphi$ was compared with that corresponding to $\varphi = 0$ (pure water), denoted as $\left(\overline{T}\right)_{\varphi=0}$. The temperature difference

$$\overline{\delta} = \left(\overline{T}\right)_\varphi - \left(\overline{T}\right)_{\varphi=0} \tag{9}$$

was determined for all treated cases and is presented in Fig. 7 versus φ for $3.25\text{x}10^6 \leq Ra \leq 4.56\text{x}10^9$ and $\alpha = 0, 90°, 180°$. It shows a clear decrease of the surface temperature when the volume fraction increases, exceeding 7K for the combination

$\left(\varphi = 10\%, \alpha = 180°, Ra = 4.56x10^9\right)$. This figure confirms the effectiveness of the nanofluid for hemispherical electronic component cooling purposes.

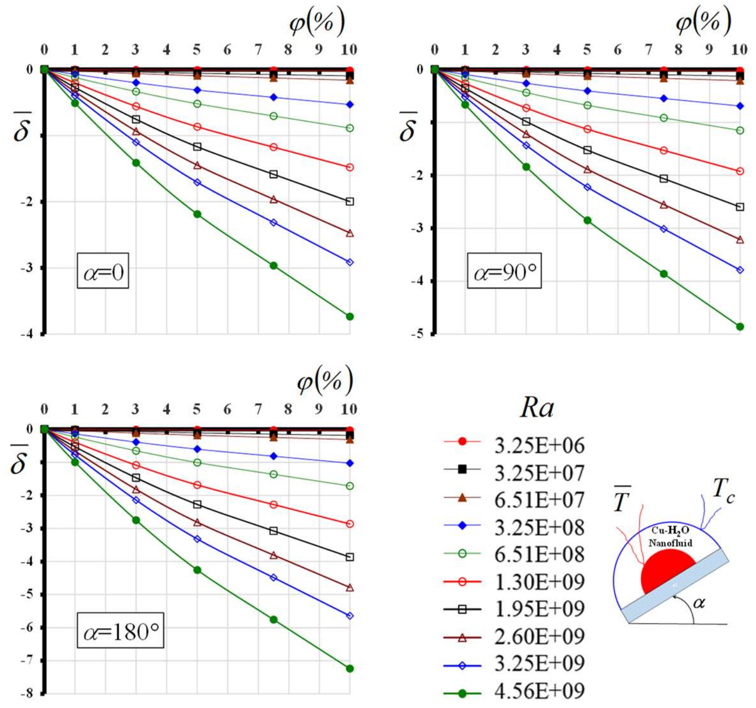

Figure 7. Evolution of the temperature difference $\overline{\delta}$ versus the volume fraction φ for $3.25x10^6 \le Ra \le 4.56x10^9$ and $\alpha = 0, 90°, 180°$

The temperature values obtained in the present study are in agreement with those of the recent study [33] which quantifies the average convective exchanges for all treated cases. The average convective heat transfer coefficient $\overline{h}$ calculated by means of the correlation of the $\overline{Nu} - Ra - \Pr$ type proposed in [33] was used in the heat balance $P = \overline{h} S_h \overline{\Delta T}$ for temperature difference $\overline{\Delta T}$ determination. The result compared with that of the present study leads to low deviations, ranging from 0.3 to 0.5% on average, with a marginal maximum deviation of 2.4% obtained for the lowest Ra value.

5. Correlations

To optimize the thermal design of the considered assembly, a correlation of the

$$\overline{\Delta T} = [k(\alpha) + b(\alpha) Ra] \Pr^{m(\alpha)} + r \quad (10)$$

type has been developed by considering the results to all the combinations treated in this study. Evolution of the (k, b, m) parameters versus α are presented in Fig. 8.

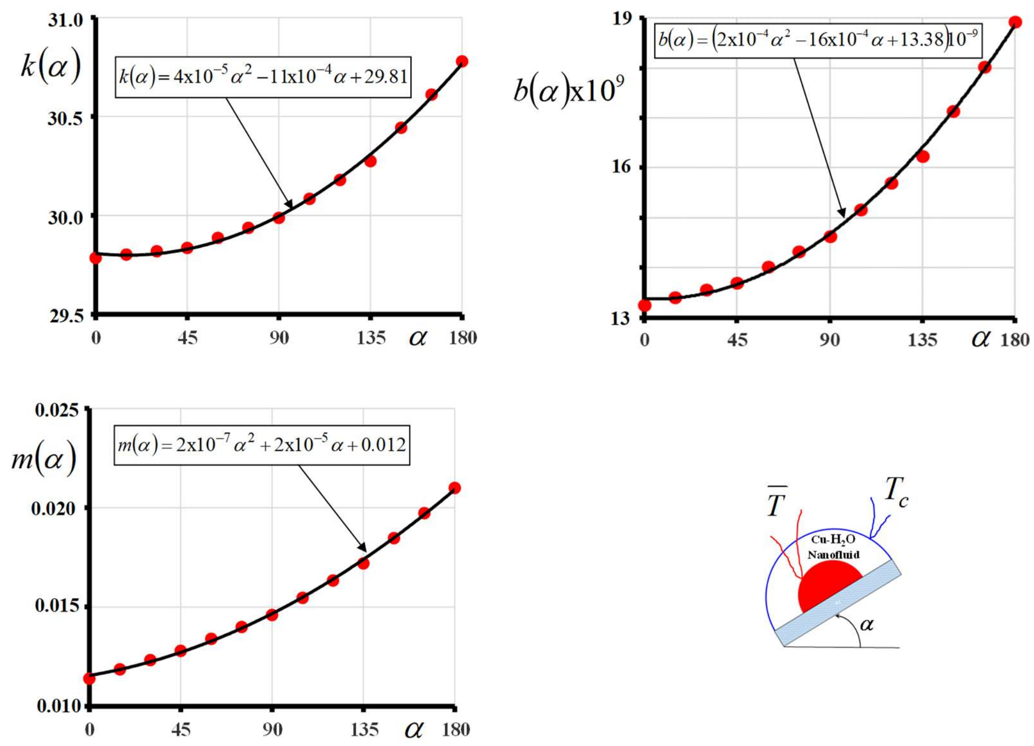

Figure 8. Evolution of the functions (k, b, m) versus the tilt angle α in the correlation

$$\overline{\Delta T} = [k(\alpha) + b(\alpha) Ra] Pr^{m(\alpha)} + r$$

The well-known least square optimization method shows that they can be represented by the second order polynomial type functions shown in the figure, whose coefficients of determination are higher than 0.998. The parameter r corresponds to the adjustment of the results with the reference temperature.

Finally, the average temperature of the active dome could be easily calculated by means of the following correlation

$$\overline{\Delta T} = \overline{T} - T_c = \left[k(\alpha) + b(\alpha)Ra\right]\mathrm{Pr}^{m(\alpha)} - 26.9$$

$$\begin{cases} k(\alpha) = 4\mathrm{x}10^{-5}\alpha^2 - 11\mathrm{x}10^{-4}\alpha + 29.8 \\ b(\alpha) = \left(2\mathrm{x}10^{-4}\alpha^2 - 16\mathrm{x}10^{-4}\alpha + 13.38\right)\mathrm{x}10^{-9} \\ m(\alpha) = 2\mathrm{x}10^{-7}\alpha^2 + 2\mathrm{x}10^{-5}\alpha + 0.012 \end{cases}$$

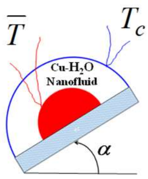

valid for (11)

$$\begin{cases} 3.26\mathrm{x}10^{6} \le Ra \le 4.56\mathrm{x}10^{9} \\ 0 \le \alpha \le 180^\circ \\ 3.255 \le \mathrm{Pr} \le 6.074 \end{cases}$$

The values of $\overline{\Delta T}$ obtained with this correlation slightly differ from those obtained through numerical approach. Relative deviations are low, varying between 0.2 and 0.6% on average. The maximum deviation of 2% corresponds to the lowest Ra value considered in the study.

6. Conclusion

The aim of this work is to examine the thermal behavior of a hemispherical electronic component. This active dome generates high power leading to Rayleigh number values reaching $4.56\mathrm{x}10^9$. It is covered by concentric cupola maintained isothermal and the space between the hemispheres is filled with a monophasic Water base-Copper nanofluid whose volume fraction varies between 0 (pure water) and 10%. The disc of the enclosure may be tilted at an angle ranging between 0° and 180° (horizontal disc with dome facing upwards and downwards). The numerical solution has been obtained by means of the volume control method based on the SIMPLE algorithm. The study shows that for some (Ra, φ, α) combinations, the temperature can reach high values with consequences such as nanofluid boiling, exceeding the maximum permissible temperature for the electronic device, early aging and even nanofluid physical state deterioration. These effects incompatible with normal operation of the electronic assembly confirm the need for thermoregulation. The surface temperature of the active component is therefore essential for thermal dimensioning of this assembly. This important data can be easily determined by means of the correlation proposed in this work valid in wide ranges of the Rayleigh number, enclosure tilt angle and nanofluid volume fraction.

References

[1] A. Baïri, J.-M. García de María, Inter Journal of Heat and Mass Transfer 66, 355-365 (2013)

[2] A. Baïri, International Communications in Heat and Mass Transfer 57, 291–296 (2014)

[3] A. Baïri, International Communications in Heat and Mass Transfer 57, 347–352 (2014)

[4] A. Baïri, Internatio Journal of Nume Methods for Heat & Fluid Flow 25 (4), 629-638 (2015)

[5] A. Baïri, International Communications in Heat and Mass Transfer 59, 174–17 (2014)

[6] Y. Shiina, K. Fujimura, T. Kunugi, N. Akino, International Journal of Heat and Mass Transfer 37(11), 1605-1617 (1994)

[7] S.D. Lee, K.Y. Suh, Journal of Nuclear Science and Technology 40 (10) 775-782 (2003).

[8] T.G. Theofanous, S. Angelini, Nuclear Engineering and Design 0200 1-9, (2000).

[9] N.S. Akbar, E.N. Maraj & A.W. Butt, Eur. Phys. J. Plus 129: 183 (2014).

[10] L. Yang, K. Dua, International Journal of Heat and Mass Transfer 108, 11–31 (2017).

[11] N.A.C Sidik, I.M. Adamu, M.M. Jamil, G.H.R. Kefayati, G. Najafi, Internat Commu in Heat and Mass Transfer 78, 68–79 (2016).

[12] Sahebi, S.A.R., Pourziaei, H., Feizi, A.R. et al. Eur. Phys. J. Plus 130: 238 (2015).

[13] M. Sheremet , I. Pop , H.F. Öztop & N. Abu-Hamdeh, Int. J. of Num. Meth. for Heat & Fluid Flow 27(4), 958-980 (2017).

[14] H.F. Öztop, P. Estellé, W-M Yan, K. Al-Salem, J. Orfi & O. Mahian, International Com in Heat and Mass Transfer 60, 37-44 (2015).

[15] M. Sabour, M. Ghalambaz & A. Chamkha, Int. Journal of Num. Meth. for Heat & Fluid Flow, https://doi.org/10.1108/HFF-12-2015-0516 (2016)

[16] M.A Sheremet & I. Pop, Eur. Phys. J. Plus 130: 107 (2015).

[17] K. Milani Shirvan, H.F. Öztop & K. Al-Salem, Eur. Phys. J. Plus 132: 204 (2017).

[18] M.A Sheremet, I. Pop & A. Shenoy, Eur. Phys. J. Plus 131: 62 (2016).

[19] A. Raisi, Applied Thermal Engineering 110, 469–480 (2017).

[20] E. Abu-Nada, International Communications in Heat and Mass Transfer 85, 1-11 (2017).

[21] E. Abu-Nada, International Journal of Thermal Sciences 50, 1720-1730 (2011).

[22] K. Khanafer, K. Vafai, M. Lightstone, Int. J. Heat Mass Transfer 46, 3639-3653 (2003).

[23] M. Sheikholeslami, M. Gorji-Bandpy, D.D Ganji, Eur. Phys. J. Plus 130: 225 (2015).

[24] M. Mamourian, K.M. Shirvan, I. Pop, Inter Com in Heat and Mass Transf 79, 46-57 (2016).

[25] G. Saha, M.C. Paul, International Com in Heat and Mass Transfer 82, 49–62 (2017).

[26] M. Corcione, Energy Conversion and Management 52, 789–793 (2011).

[27] L. Yang, J. Xu, K. Dua, X. Zhang, Powder Technology 317, 348–369 (2017).

[28] A. Shahsavar, M. Bahiraei, Powder Technology 318, 441–450 (2017).

[29] N.N. Esfahani, D. Toghraie, M. Afrand, Powder Technology 323, 367–373 (2018).

[30] A. Huminic, G. Huminic, C. Fleaca, F. Dumitrache, I.Morjan, Powder Technology 284, 78–84 (2015).

[31] O. Haddad, A. Baïri, N. Alilat, J.G. Bauzin, N. Laraqi, Interna Com in Heat and Mass Transfer 87, 204–211 (2017).

[32] A. Baïri, O. Haddad, N. Alilat, Numerical Heat Transfer 71(11) 1094-1103 (2017).

[33] A. Baïri, Natural convection between concentric and inclined hemispherical cavities filled with Cu-Water nanofluid, Seminar on Heat Transfer and Engineering Applications, Universidad del Pais Vasco (Spain), Proc. TMHC-HTEA 4423, Paper 016/ 05-07 June 2017, pp. 76-85.

[34] A. Baïri, International Communications in Heat and Mass Transfer 57, 347–352 (2014).

[35] S.V. Patankar, Numerical Heat Transfer and Fluid Flow, series in computational methods in mechanics and thermal science, Taylor and Francis Publishers, W.J. Minkowycz and E. Sparrows, Editors, ISBN 0-89116-522-3, 1980.

[36] A. Bejan, Convection Heat Transfer, fourth ed., John Wiley & Sons, Inc., Hoboken, NJ, USA, 2013 http://dx.doi.org/10.1002/9781118671627.

[37] K.S. Hong, T.K. Hong, H.S. Yang, Appl. Phys. Lett. 88 (3), 1–3 (2006).

[38] S. Hassani, R. Saidur, Saad Mekhilef, Arif Hepbasli, Internat Jour of Heat and Mass Transfer 90, 121–130 (2015).